JOURNAL OF MATERIALS SCIENCE 10 (1975) 453–459

Deformation and fracture of an amorphous metallic alloy at high pressure

L. A. DAVIS, S. KAVESH
Materials Research Center, Allied Chemical Corporation, Morristown, NJ, USA

The influence of hydrostatic pressure ($\sim$ 6.5 kbar) on the stress for plastic flow in a $Pd_{77.5}Cu_6Si_{16.5}$ amorphous metallic alloy in compression and tension has been examined. The observed effect ($\Delta \ln\sigma/\Delta P \simeq 5 \times 10^{-6}$ bar^{-1}) is very close to that exhibited by crystalline metals. The highly inhomogeneous nature of the deformation appears to be unaltered by pressure. As at one atmosphere, failure in tension with high superposed pressure occurs by rupture through a zone of intense plastic shear. The fracture surface topography is strikingly different, however, because cracking inside the shear zone is suppressed in favour of crack initiation at its periphery.

1. Introduction

A number of characteristic feature sof the mechanical behaviour of amorphous metallic alloys are now well established. Typically, for example, these materials exhibit high strengths. For alloys based on Pd tensile strengths of the order of 150 kg mm^{-2} may be observed [1, 2], while for alloys based on Ni and/or Fe tensile strengths on the order of 140 to 280 kg mm^{-2} are observed [3, 4]. This strength is accompanied by good ductility in the sense that wires or ribbons may be sharply bent back on themselves without rupture [2, 5]. During loading in uniaxial tension or compression, near ambienl conditions, the deformation of these materiats occurs in highly inhomogeneous localized shear bands. In compression many intense, intersecting slip bands are active [6, 7], but in tension a singularly intense shear band develops and failure occurs at low elongation by shear rupture, i.e. fracture proceeds through the intense shear zone [1-4].

The temperature dependence of the flow and fracture of metallic glasses was examined by Masumoto and Maddin [1] and by Pampillo and Polk [3, 4]. The observed behaviour is relatively insensitive to glass composition and is similar to that observed for crystalline metals [4]. That is, the shear strength τ varies in proportion to the shear modulus G over an intermediate temperature range ($\sim$ 250 to 400 K for metallic glasses). At lower temperatures, τ increases more rapidly than G with decreasing T and at higher temperatures it decreases more rapidly with increasing T [4]. The stress relaxation and creep behaviour of a metallic glass ($Pd_{80}Si_{20}$) have also been observed [8].

No observations have been made, however, regarding the influence of superposed hydrostatic pressure on the mechanical properties of metallic glasses. For crystalline metals at ambient temperature, where plastic flow is typically athermal, the influence of pressure on the stress for plastic flow (σ) is small; σ increases in proportion to the pressure dependence of the shear modulus [9]. Given the athermal behaviour of metallic glasses at ambient temperature one may expect that a similarly small effect will be observed for them. On the other hand Bridgman [10] has demonstrated the profound effect of hydrostatic pressure on the tensile failures of crystalline materials when void formation is required. Hence the relative importance of dilatation in the shear rupture of a metallic glass may be examined. We examine here the influence of pressure on the flow and fracture of a $Pd_{77.5}Cu_6Si_{16.5}$ amorphous alloy. The subscripts represent atomic percentages.

2. Experimental procedure

2.1. Mechanical testing apparatus

Detailed descriptions of the high-pressure mechanical testing apparatus (minitester) have been given elsewhere [11-13]. It will suffice here to note that the apparatus is a miniature, synchronous motor-driven device which operates

completely enclosed in a high pressure vessel. An internal strain-gauge type load cell is employed to measure load. The dependence of the cell calibration factor on pressure is determined using a stiff steel spring as a standard. The axial deformation rate generated by the tester is determined by the frequency of the power supplied to the motor, the gear reduction employed and the pitch of the drive screw. For the present experiments a displacement rate of 9.53×10^{-3} cm min^{-1} was used. The minitester is capable of generating a maximum load of about 225 kg. As a practical matter specimens are scaled to limit the load required for deformation to about 100 kg. The configuration of the tester is such that no sliding guides are interposed between the sample and load cell. Hence the influence of frictional effects on the measured load is excluded.

2.2. Pressure system

The minitester operates enclosed in a liquid medium, 14 kbar capacity, Harwood pressure system [14]. The pressure fluid employed was *n*-pentane. Pressure is monitored by a manganin cell with an accuracy of $\sim 1\%$. All experiments were conducted at room temperature ($\sim 22°C$) and sufficient time was allowed (> 10 min) after pressurization for the heat generated by compression of the fluid to be dissipated into the massive steel pressure-vessel.

2.3. Tension

Filaments of $Pd_{77.5}Cu_6Si_{16.5}$ of about 0.3 mm diameter were prepared by rapid quenching from the melt. This alloy is readily quenched in the amorphous state [15] and the present samples were confirmed to be amorphous by X-ray diffraction examination.

The filaments were tested as produced, i.e. without surface treatment, using drum-clamp type grips. A specimen is wrapped on the drums and exits them tangentially along the centre axis of the loading system. Arrangement of the clamps is such that the specimen is not clamped at the tangents. The initial tangent to tangent distance is set at 2.54 cm. For the displacement rate given above this provides a tensile strain rate of $\sim 6.3 \times 10^{-5}$ sec^{-1}.

2.4. Compression

A cast rod of $Pd_{77.5}Cu_6Si_{16.5}$, prepared by Pampillo and Chen [6], was centreless ground to a diameter of ~ 2 mm; three specimens were cut to lengths of ~ 4 mm. To scale the specimen cross-section to a suitable size, a gauge section of ~ 0.84 mm diameter and ~ 1.1 mm length (slightly hour-glass shaped) was centreless ground on each specimen. For the deformation rate noted above this yields a compressive strain rate of $\sim 1.45 \times 10^{-3}$ sec^{-1}.

3. Results

3.1. Compression

The influence of hydrostatic pressure on the compressive plastic deformation of $Pd_{77.5}Cu_6Si_{16.5}$ was determined in an interrupted type of test, i.e. a sample is loaded to initiate plastic flow at 1 atm, the load is then removed and the system is pressurized and, finally, plastic deformation is reinitiated at high pressure. The result is shown in Fig. 1. The observed serrated flow is typical of this alloy [6, 7] and does not appear to be significantly affected by high pressure. The apparent rate of work hardening appears slightly reduced at high pressure, but this is probably an artifact associated with the mildly rounded load-compression curve observed for this material [6, 7]. The observed dependence of the flow stress on pressure, $\Delta \ln\sigma/\Delta P$, is $5 \pm 0.7 \times 10^{-6}$ bar^{-1}, i.e. σ increases by about 0.5% per kbar. The value given is the result of six determinations with increasing and decreasing pressure between 1 atm and 6.2 kbar on three specimens; the limits represent the average deviation from the mean value. The estimated absolute uncertainty, which derives from the uncertainty in determination of the pressure dependence of the load cell calibration is $\sim \pm 1 \times 10^{-6}$ bar^{-1}.

At large deformation the specimens fail by shearing off. The area of this shear plane was measured for the specimen of Fig. 1 and the flow stress thereby estimated. The calculated plateau compressive stress is ~ 154 kg mm^{-2}, which compares with a value of ~ 160 kg mm^{-2} estimated from the data of Pampillo and Chen [6] for cylindrical specimens.

3.2. Tension

Typical stress-strain curves in tension for $Pd_{77.5}Cu_6Si_{16.5}$ are shown in Fig. 2. Small serrations on each curve are clearly evident prior to failure. Four samples each, were deformed to fracture at 1 atm and 6.9 kbar. The observed fracture stresses were 146.6 ± 2.5 kg mm^{-2} and 151.8 ± 1.8 kg mm^{-2}, respectively, where the limits represent the average deviation

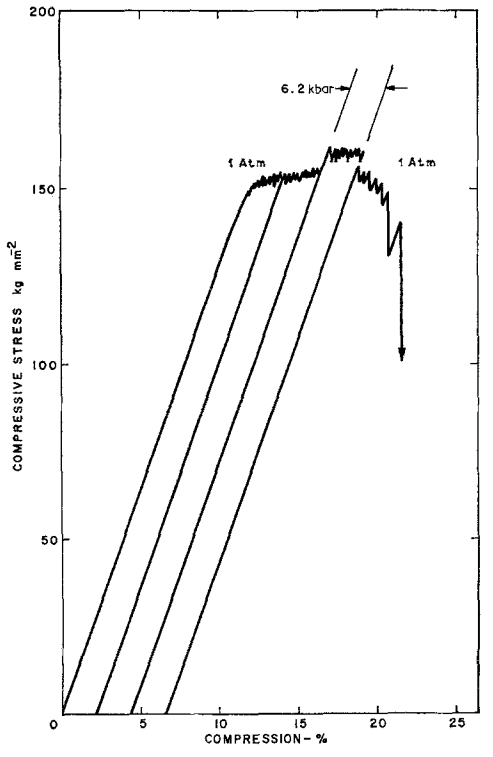

Figure 1 Compressive stress versus nominal compressive strain for amorphous $Pd_{77.5}Cu_6Si_{16.5}$, exhibiting the effect of pressure on the stress for plastic flow. The elastic portion of each curve reflects the stiffness of the tensile machine rather than the inherent stiffness of the material.

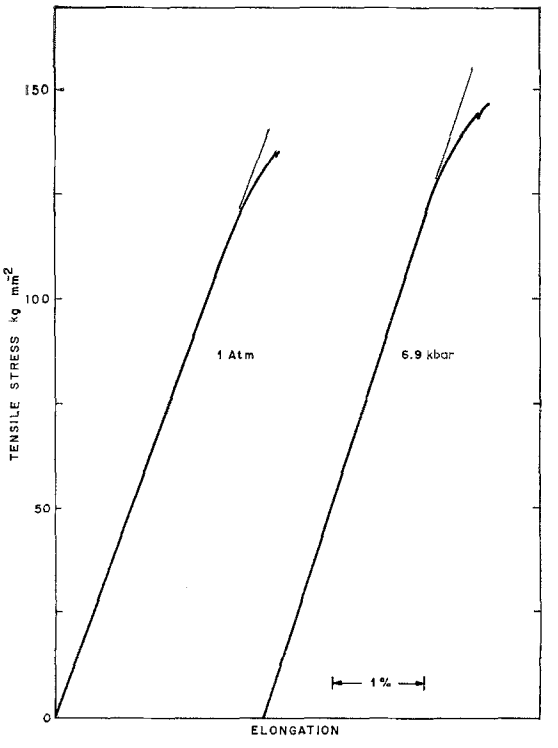

Figure 2 Typical tensile stress versus elongation curves (based on a 25.4 mm gauge length) for amorphous $Pd_{77.5}Cu_6Si_{16.5}$ at 1 atm and 6.9 kbar.

from the mean value. Based on these data the pressure coefficient of the *fracture stress*, $\Delta \ln \sigma_f / \Delta P$ also equals $\sim 5 \times 10^{-6}$ bar^{-1}.

Optical examination of the specimens indicates that failure usually occurs near one of the grips, i.e. near where the specimen parts contact with the drum tangentially, as shown schematically (edge on profile) in Fig. 3a. The fracture surface lies perpendicular to the plane of the figure and hence approximately parallel to the axis of the drum; the shear direction is parallel to the figure and at $\sim 45°$ to the specimen axis.

According to Pampillo and Chen [6] intersecting shear bands appear to occur at 45° to the deformation axis in compression. Accordingly, the same angle is to be expected for tension. The fracture tips, however, are curved as shown schematically in edge profile in Fig. 3b; the top piece exhibits an average angle of $\sim 50°$ to the tensile axis, while the bottom piece exhibits the complementary angle of $\sim 40°$. This behaviour occurs because deformation is confined to a single "slip system" as in a single crystal. Hence

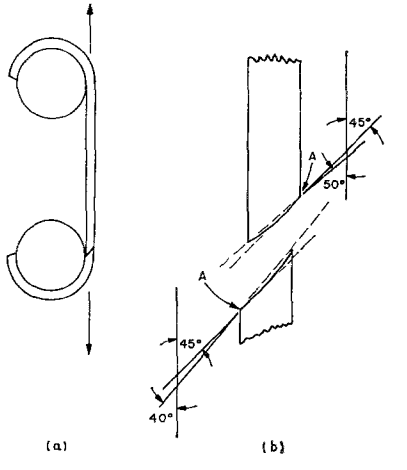

Figure 3 (a) Schematic representation of the configuration of tensile failure relative to the loading grips. (b) Schematic representation of the distortion of the specimen tips which results due to bending.

the slip directions (originally at 45° to the tensile axis on a 45° plane) must rotate towards the tensile axis. The lateral constraint of the grip

prevents free rotation [17] and the observed distortion results, owing to bending.

It is also observed that shear steps, such as those in Fig. 4, appear on the sample only over a distance of $\sim$ 1 to 2 mm centred about the fracture site. Hence the "true" axial strain rate is of the order of 10^{-3} sec^{-1} and the "local" elongation to failure is $\sim$ 3 to 6%, as opposed to $\sim$ 0.27% for the total specimen. Such values are of questionable meaning, however, given the highly localized shear deformation observed.

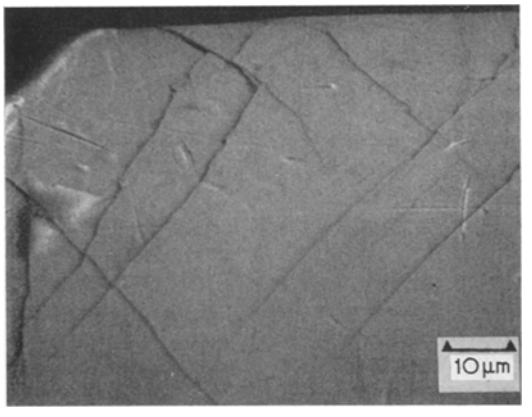

Figure 4 Shear steps isolated near the tensile fracture surface (edge at upper left) of amorphous $Pd_{77.5}Cu_6Si_{16.5}$; scanning electron micrograph.

Fig. 5 shows a scanning electron micrograph of the fracture surface of a $Pd_{77.5}Cu_6Si_{16.5}$ filament pulled to failure at 1 atm and 22°C. In this view the fracture surface is inclined $\sim$ 45° from horizontal. The nature of the surface features observed are as previously described by Leamy *et al.* [2] and Pampillo and Reimschuessel [16]. A smooth region at the periphery of the specimen (an arc centred about the shear direction at points A on opposite halves of the specimen in Fig. 3b) demarks the region of shear deformation prior to failure. A distinctive pattern, called a vein pattern [2], is observed as a network of protrusions on the otherwise smooth rupture surface, i.e. the veins do not appear to be steps in the manner of cleavage river pattern [16]. Closely matching vein patterns appear on the opposite fracture halves. The local shear strain to failure, taking the bandwidth as $\lesssim$ 1 μm (Fig. 4), is of the order of 10 or more.

The fracture surface of a specimen pulled to failure at 6.9 kbar and 22°C is shown in Fig. 6, as observed by SEM. Two distinctive features are

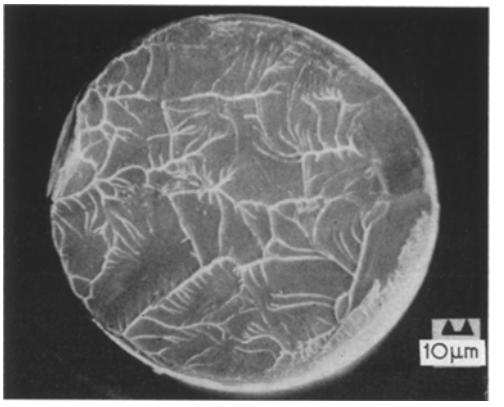

Figure 5 Fracture surface of a $Pd_{77.5}Cu_6Si_{16.5}$ filament tested at 1 atm. The direction of view is parallel to the specimen axis. The smooth shear offset region is an arc on the right of the micrograph (the "brush" markings in the shear region are an artifact caused by handling) and hence the fracture surface slopes down from left to right at an angle to the specimen axis of $\sim$ 45° (see text).

apparent: (1) the shear displacement prior to rupture is about two to three times that which obtains at 1 atm, and (2) the veins no longer exhibit the rather equiaxed features typical of 1 atm fracture (Fig. 5). Rather they tend to lie perpendicular to the shear direction and most of them appear to connect with the external surface of the specimen. The angle of the surface is as discussed for 1 atm deformation.

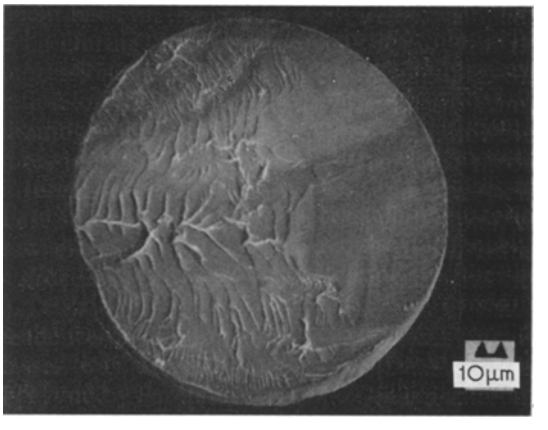

Figure 6 Fracture surface of a $Pd_{77.5}Cu_6Si_{16.5}$ filament tested at 6.9 kbar. The direction of view is parallel to the specimen axis. The shear offset region is on the right of the micrograph so that the surface slopes at $\sim$ 45° from left to right.

An effort was made to avoid the grip influence in tensile deformation; the centre section of

several filaments was reduced in diameter to $\sim$ 0.23 mm over a length of $\sim$ 8 mm by electropolishing. On elongation these specimens failed at one of the fillets at stresses equal to or less than those observed for uniform cross-section filaments. The elastic constraint supplied by the fillet is apparently approximately equivalent to that provided by the grip for uniform specimens.

4. Discussion

4.1. Tensile load-elongation curve

The occurrence of such highly localized shear deformation as exhibited in Figs. 4 to 6 is evidence that little or no work hardening accompanies deformation of metallic glasses. Hence the apparent high rate of work hardening exhibited in Fig. 2 is not inherent in the material. Rather it derives from the particular geometry of failure indicated in Fig. 3. Deformation is initiated at the grip due to the elastic constraint which obtains there. As slip proceeds on a single "slip system" the slip direction and slip plane must rotate toward the tensile axis, as noted above. This is opposed by the lateral constraint of the grip so that near the grip a bending moment is generated about an axis perpendicular to both the tensile axis and the slip direction. This moment produces a shear stress on the slip plane which opposes the "applied" shear stress [17]. Hence the applied load must continually increase in order for slip to proceed. In the absence of prior failure the load would increase to a level where the inherent yield stress of the material would be reached. Coincident yielding and failure would then occur. The fact that the load does not rise this high is evidenced by the observation that failure occurs at the grips before large shear offsets develop in the rest of the sample.

In the compression test, early deformation occurs owing to stress concentrating defects such as surface asperities, slight lack of parallelness, etc. As these sources are exhausted the stress continues to rise and reaches a plateau which, we expect, is a true measure of the compressive yield strength of the material, in this case $\sim$ 154 kg mm^{-2}.

4.2. Pressure dependence of the stress for plastic flow

From an interrupted type of deformation test one obtains directly the dependence of the flow stress on the variable in question [18], e.g. T, P or $\dot{\epsilon}$. Any further stress difference (for a given true strain) between the respective continuous stress-strain curves must be attributed to the T, P or $\dot{\epsilon}$ dependence of work hardening, i.e. to the different defect structures generated by deformation. For metallic glasses work hardening appears absent so that the dependence of flow stress on $P(\Delta \ln\sigma/\Delta P)$ could be obtained from continuous compression curves. Given the slight variation from sample to sample, however, the interrupted test allows greater experimental precision.

For the case of tension (Fig. 2) artificial work hardening does occur. Allowing for the slight increase of elongation at high pressure ($\sim$ 6% more) and the consequent slight increase of fracture load, a small correction may be applied to $\Delta \ln\sigma_f/\Delta P$ to find the pressure dependence of the flow stress. This correction is $\sim 5 \times 10^{-7}$ bar^{-1} so that $\Delta \ln\sigma/\Delta P \simeq 4.5 \times 10^{-6}$ bar^{-1}, in close agreement with the value found in interrupted compression (5×10^{-6} bar^{-1}).

The dependence of the compressive and tensile flow (or yield) stresses on pressure indicates that the yield stress in compression should exceed that in tension. Due to the grip influence in the tensile test one cannot observe this effect directly. On the other hand, one may estimate the inherent tensile yield stress on assuming that the yield stresses in tension (σ_T) and compression (σ_C) at 1 atm ambient pressure dependent linearly on the hydrostatic component of the stress tensor. Taking both σ_C and σ_T as positive,

$$\sigma_C/\sigma_T = [3 + (\Delta\sigma/\Delta P)]/[3 - (\Delta\sigma/\Delta P)]\,. \quad (1)$$

From above, $\sigma_C^{-1}(\Delta\sigma/\Delta P) \simeq 5 \times 10^{-6}$ bar^{-1} $= 4.9 \times 10^{-4}$ (kg mm^{-2})$^{-1}$; with $\sigma_C \simeq 157$ kg mm^{-2}, $\Delta\sigma/\Delta P \simeq 0.077$, $(\sigma_C/\sigma_T) \simeq 1.053$ and $\sigma_T \simeq 149$ kg mm^{-2}. Hence it appears that tensile fracture occurs at a nominal stress only slightly below the inherent yield stress of the material.

One may also suppose that shear flow is sensitive to the normal stress on the shear plane, as in a soil. In this case, according to the Coulomb criterion,

$$S = k + \mu\sigma_n \quad (2)$$

where S is the shear resistance of the material, k is the shear strength in pure shear and σ_n is the normal stress on the shear plane. Also $\mu = \tan\phi = -1/\tan 2\theta$, where ϕ is determined from the Mohr circle diagram and θ is the angle between the loading axis and the normal to the slip plane [19]. The Mohr circle diagram of Fig. 7 yields $\phi \simeq 2.5°$, $\mu = 0.044$ and $\theta \simeq 46.25°$. As one cannot reliably determine such a small

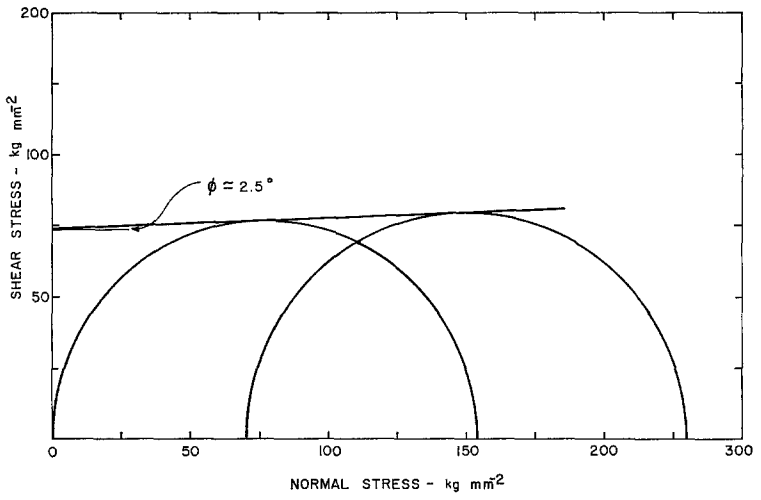

Figure 7 A Mohr circle diagram for $Pd_{77.5}Cu_6Si_{16.5}$.

deviation from 45° in experiments such as those of [6], we are unable to distinguish here between a normal stress dependence and a hydrostatic pressure dependence of the yield or flow stress.

4.3. Relevance to mechanisms of plastic flow

As discussed by Gilman [20, 21] and Li [22] plastic flow in metallic glasses presumably occurs via a dislocation mechanism. Li considers that an amorphous material may be modelled by a dislocation lattice. The shear resistance to the motion of a dislocation within this dislocation lattice is predicted, as for crystalline materials, in terms of the shear modulus, G. Accordingly, assuming athermal behaviour, one would expect $\Delta \ln\sigma/\Delta P \simeq \Delta \ln G/\Delta P$.

Gilman considers the flow behaviour of a metallic glass as analogous to the behaviour of a soil. A quantitative model is developed in which the resistance to plastic shear is related to the core dilatation which accompanies dislocation motion. Spaepen and Turnbull [23] consider, qualitatively, the local dilatation associated with the elastic-plastic boundary of a propagating shear zone. Gilman's treatment leads to $\Delta \ln\sigma/\Delta P \simeq (4/5)\Delta \ln G/\Delta P + (1/5)\Delta \ln B/\Delta P$, and that of Spaepen and Turnbull suggests $\Delta \ln\sigma/\Delta P \simeq \Delta \ln B/\Delta P$, where B is the bulk modulus.

On the basis of the present data one might hope to distinguish between these models. Unfortunately, however, no data are presently available for the pressure dependence of G or B for metallic glasses. Also for crystalline metals such as Fe, Ni, Cu and Al, it is observed that $\Delta \ln B/\Delta P \approx \Delta \ln G/\Delta P \approx 5 \times 10^{-6}$ bar$^{-1} \approx \Delta \ln\sigma/\Delta P$ [9, 24]. Hence the observed pressure dependence of the flow stress for metallic glasses is consistent with that for crystalline metals, but if the analogy is completed, the relative increases of B and G with pressure for metallic glasses might be approximately equivalent.

4.4. Tensile fracture

Pampillo and Reimschuessel [16] have discussed in some detail the tensile fracture surface features (1 atm) of amorphous $Pd_{77.5}Eu_6Si_{16.5}$. As observed in Fig. 5 a relatively coarse vein pattern is observed at 1 atm. As failure occurs through the shear zone it appears that the veins are intersections of shear disc cracks originating from multiple nucleation sites. The cracks expand, depending on the location on their periphery, by pure shear, ductile tearing and all combinations in between. (An analogy to the expansion of a dislocation loop is appropriate.) The cracks may expand in a uniform fashion to produce broad, clear areas or they may become unstable so that "finger" cracks run into the material. Within a given disc shaped zone this produces a finer system of veins, all of which point toward the nucleus of a local crack.

The typical failure topography of a specimen fractured at 6.9 kbar (Fig. 6) is strikingly different from that observed at 1 atm. The shear offset prior to failure is several times larger. Apparently the local defects, which might be, for example, small voids, inclusion particles or isolated crystalline regions, which nucleate cracks in the shear zone at 1 atm are ineffective

at high pressure. Clearly such crack formation must have a dilatational component which is opposed by the superposed hydrostatic compressive stress field. Shear displacement, therefore, proceeds until the "notch" created by the shear offset itself is effective in nucleating cracks at the periphery of the specimen. Such cracks bow out over small distances and prefer to run from the periphery in the pure "screw" mode, i.e. perpendicular to the slip direction. Hence the fracture surface is marked with closely spaced veins approximately perpendicular to the slip direction.

5. Conclusion

Amorphous $Pd_{77.5}Cu_6Si_{17.5}$ exhibits a modest pressure dependence of plastic flow ($\Delta \ln\sigma/\Delta P \simeq 5 \times 10^{-6}$ bar^{-1}) very close in magnitude to that observed in crystalline metals. Based on this pressure (or normal stress) dependence one may expect the yield stress in compression to exceed that in tension. Owing to the elastic constraint provided by the grips in a tensile test one cannot observe this effect directly. One may estimate, however, that the inherent yield stress in tension ($\sim$ 149 kg mm^{-2}) is only slightly greater than the observed fracture stress ($\sim$ 146 kg mm^{-2}).

Tensile failure at 1 atm is initiated by the formation and dilatation of shear disc type cracks within the intense shear zone. Under the influence of superposed hydrostatic pressure this process is suppressed. Hence the observed shear displacement prior to fracture is greater and failure is initiated by cracks running from the periphery of the shear zone.

Acknowledgements

Thanks are due to Mrs Annemarie Reimschuessel for her co-operation in use of the scanning microscope, to Miss Patricia Brady for her assistance with the microscopy, and to Mr Richard Fehrman for his assistance with the mechanical testing.

References

1. T. MASUMOTO and R. MADDIN, *Acta Metallurgica* **19** (1971) 725.
2. H. J. LEAMY, H. S. CHEN and T. T. WANG, *Met. Trans.* **3** (1972) 699.
3. D. E. POLK and C. A. PAMPILLO, *Scripta Metallurgica* **7** (1973) 1161.
4. C. A. PAMPILLO and D. E. POLK, *Acta Metallurgica* **22** (1974) 741.
5. H. S. CHEN, H. J. LEAMY and M. J. O'BRIEN, *Scripta Metallurgica* **7** (1973) 415.
6. C. A. PAMPILLO and H. S. CHEN, *Mat. Sci. Eng.* **13** (1973) 181.
7. H. S. CHEN, *Scripta Metallurgica* **7** (1973) 931.
8. R. MADDIN and T. MASUMOTO, *Mat. Sci. Eng.* **9** (1972) 153.
9. P. HAASEN and A. W. LAWSON, *Z. Metallk.* **49** (1958) 280.
10. P. W. BRIDGMAN, "Studies in Large Plastic Flow and Fracture" (McGraw-Hill, New York, 1952) p. 76.
11. R. B. GORDON and L. MIKE, *Rev. Sci. Instrum.* **38** (1967) 541.
12. L. A. DAVIS and R. B. GORDON, *J. Appl. Phys.* **39** (1968) 3885.
13. L. A. DAVIS and C. A. PAMPILLO, *ibid* **42** (1971) 4659.
14. HARWOOD ENGINEERING CO, Walpole, Mass., USA.
15. H. S. CHEN and D. TURNBULL, *Acta Metallurgica* **17** (1969) 1020.
16. C. A. PAMPILLO and A. C. REIMSCHUESSEL, *J. Mater. Sci.* **9** (1974) 718.
17. R. L. FLEISCHER and B. CHALMERS, *J. Mech. Phys. Solids* **6** (1958) 307.
18. A. H. COTTRELL and R. J. STOKES, *Proc. Roy. Soc. (Lond.)* **A233** (1955) 17.
19. A. H. COTTRELL, "The Mechanical Properties of Matter" (Wiley, New York, 1964) p. 315.
20. J. J. GILMAN, *J. Appl. Phys.* **44** (1973) 675.
21. *Idem*, to be published.
22. J. C. M. LI, to be published in "Distinguished Lectures in Materials Science" (Marcel-Dekker, New York, 1974).
23. F. SPAEPEN and D. TURNBULL, *Scripta Metallurgica* **8** (1974) 563.
24. A. SEEGER and P. HAASEN, *Phil. Mag.* **3** (1958) 470

Received 29 August and accepted 9 September 1974.